H. R. Salimi Jazi
Department of Materials Engineering,
Isfahan University of Technology,
Isfahan 84156-83111, Iran;
Centre for Advanced Coating Technologies,
University of Toronto,
Toronto, M5S 3G8, Canada

J. Mostaghimi

S. Chandra

L. Pershin

T. Coyle

Centre for Advanced Coating Technologies,
University of Toronto,
Toronto, M5S 3G8, Canada

Spray-Formed, Metal-Foam Heat Exchangers for High Temperature Applications

Open pore metal foams make efficient heat exchanger because of their high thermal conductivity and low permeability. This study describes a novel method of using wire-arc spraying to deposit Inconel 625 skins on the surface of sheets of 10 and 20 pores per linear inch nickel foam. The skins adhere strongly to the foam struts, giving high heat-transfer rates. Tests were done to determine the hydraulic and thermal characteristics of the heat exchangers and correlations developed to calculate Fanning friction factor and Nusselt number as a function of Reynolds number for airflow through the foam. Measured heat-transfer coefficients for the foam heat exchangers are greater than those of straight flow channels at the same flow rate. A ceramic thermal barrier coating was deposited on one face of the heat exchanger using plasma spraying. The coating and heat exchanger survived prolonged exposure to the flame of a methane-air burner.
[DOI: 10.1115/1.4001049]

1 Introduction

Many processes have been developed in recent years to manufacture metallic foams with both open (interconnected) and closed pores [1]. Such porous metals combine low weight with high strength, making them useful in a number of applications such as lightweight structural components, acoustic insulation, energy absorption systems, and vibration dampers. Metal foams also have large internal surface area and high thermal conductivity and, recently, there has been interest in finding use for open-pore metal foams as heat exchangers [2], heat sinks [3], boilers [4], burners [5], and filters [6]. The high permeability of the foams to fluid flow and their large surface area yield high heat-transfer rates with low pressure drops.

Boomsma and Poulikakos [7] and Dukhan and Chen [8] measured pressure drops across aluminum foams with air flowing through them and used equations developed for flow through porous media to correlate their results. Banhart [1] measured pressure drops for both air and water flowing with a wide range of Reynolds numbers through various foams made from differing materials and with a variety of pore sizes and showed that average pore size is sufficient to predict pressure drop.

Gibson and Ashby [9] proposed using metal foams as compact heat exchangers and developed an analytical heat-transfer model in which foam struts were idealized as cylinders in cross-flow. Boomsma et al. [2] measured heat-transfer from a heated aluminum foam to air flowing through it and found it to be two to three times higher than those in commercially available heat exchangers while using the same pumping power. Dukhan and Chen [8] did experiments on internal forced convection to air blown through metal foam sheets heated on one face and developed a model to predict their results.

To make a heat exchanger, a shell has to be placed on the external surfaces of the foam structure to confine the fluid flowing within. Heat is conducted through the foam struts to the exterior casing and then to the surroundings. Various manufacturing processes such as cladding, brazing, and diffusion bonding of metal sheets have been used to attach skins to the surfaces of metal foams. All of these are not only relatively expensive processes but they also have a more serious shortcoming: They bond only a relatively small fraction of struts to the outer sheath. Thermal resistance at the strut-skin interface therefore limits heat-transfer. If the heat exchanger surface is curved, or has a more complex shape with cavities in it, bonding a skin is even more difficult.

The objective of this study was to make compact heat exchangers, using a novel method of depositing skins on the surfaces of foams, and to test their performance. Our goal was to make a high-temperature heat exchanger, capable of withstanding the thermal shock of combustion gases on one of its exterior faces while being cooled by air flowing through it.

In this paper we describe a method of depositing casings on the surface of open-pore metal foam sheets using thermal spray coating processes in which powders or wires of the coating material are fed into a high-temperature, high velocity gas jet, melted and accelerated toward the substrate. A spray of molten powder particles impact on the substrate, where they flatten and solidify after impact, coalescing with each other to form a thin, dense layer. By manipulating the thermal spray gun and substrate using a robot, sheaths can be deposited on the surface of structures with complicated shapes. Because the skins are formed by the solidification of molten droplets they are welded to each strut, making good mechanical and thermal connections.

We developed a new method to deposit skins on the surface of nickel foams in which surface pores in the foam were filled with a paste made from a mixture of resin and powder particles. The surface was then grit blasted to expose the tips of foam struts and a layer of Inconel 625 (an oxidation resistant alloy of Ni 58%, Cr 20–23%, Mo 8–10%, Fe 5%, Nb 3–4%) was deposited on the metal foam sheet using a wire-arc spray process. To make one surface resistant to combustion temperatures a layer of ceramic (yttria stabilized zirconia (YSZ), which is ZrO_2 containing 7% Y_2O_3) was deposited on top of the metallic skin using atmospheric plasma spraying. A detailed study was conducted of the metallurgical and microstructural characteristics of the skins and the mechanical properties of the sandwich structure and has been reported elsewhere [10–12].

Rectangular channels made of nickel foam cores with Inconel 625 skins deposited by thermal spray were placed on a heater block while cooling air was blown through them. We measured pressure drop and temperature rise of air while varying flow rate. The data were used to calculate dimensionless parameters such as

Contributed by the Heat Transfer Division of ASME for publication in the JOURNAL OF THERMAL SCIENCE AND ENGINEERING APPLICATIONS. Manuscript received July 1, 2009; final manuscript received January 7, 2010; published online April 6, 2010. Assoc. Editor: Arun Muley.

Table 1 APS and wire-arc spray process parameters

Parameter	APS	Wire arc
Spray torch	SG-100	ValuArc
Coating material	YSZ	Inconel 625
Feed rate, g/min	6	82
Spray distance, mm	60	100
Current, A	750	200
Voltage, V	60	33
Total gas flow rate, (Ar/He), slpm	50/1	-

Reynolds number, Nusselt number, and Fanning friction factor that are conventionally used to describe heat exchanger performance.

2 Heat Exchanger Fabrication

Sheets of open cell nickel foam (Inco Special Products, Mississauga, Canada) were cut into rectangular sheets, 220×100 mm^2 in size. Sheets with three pore sizes were used: 10 pores per linear inch (PPI, with pore diameter of 2–3 mm); 20 PPI (pore diameter of 1–2 mm); and 40 PPI (pore diameter of 0.2–0.5 mm). Sheets were available in thicknesses of 3 mm or 10 mm and thinner sheets could be fused together to form thicker layers by diffusion bonding by stacking them under a load of 15 g/cm^2 in a furnace at 1200°C for 2 h.

It is impossible to directly spray skins on the surface of metal foams since molten particles in a thermal spray (typically 20–40 μm in diameter) easily penetrate into foam through open pores, which are more than an order of magnitude larger. A new process was developed to deposit a dense, strongly adhering skin onto the surface of a foam sheet using thermal spray processes, irrespective of its pore size and density. The penetration of the coating materials into the foam substrates was controlled by filling surface pores with a paste prepared from a mixture of a thermoset resin and Inconel 625 powder particles. The paste was spread over the surface of the foam, penetrating to a depth of 1–2 mm. The paste was cured at ~200°C for ~2 h and then the filled foam surface grit blasted to remove extra paste and roughen the surface. Grit blasting also exposed the tips of the foam struts, allowing the sprayed skin to adhere strongly.

Skins with an average thickness of 400 μm were deposited on all sides of the foam samples using a twin wire-arc spraying system (ValuArc, Sulzer Metco Inc., Westbury, NY) and Inconel 625 (Plasma Powder & Systems, NJ). In some cases a thermal barrier coating (TBC) was deposited on one face of the heat exchanger using atmospheric plasma sprayed (APS) yttria stabilized zirconia powder (ZrO_2-7%Y_2O_3, Amperit 825-0, H.C. Starck, Germany) applied with a SG 100 plasma gun (Praxair, Mississauga, ON, Canada). The coating thickness was around 300 μm. The spray process parameters for different spray processes are listed in Table 1. After coatings were applied samples were heat treated in a furnace under vacuum condition at 1150°C for 2 h to relieve residual stresses and burn away any remnants of the resin used to fill surface pores.

Figure 1 shows samples of a 20 PPI Ni foam (Fig. 1(*a*)) and two foam samples on which a ceramic (lower sample) or metallic (upper sample) coating has been applied. Figure 2(*a*) shows a cross-section through the skin on the 40 PPI nickel foam substrate. The deposit consists of an ~300 μm thick layer of Inconel 625 deposited by twin wire-arc, spraying on top of which, is an ~400 μm thick YSZ coating deposited by atmospheric plasma spraying. Figure 2(*b*) shows an enlarged view of a foam strut: the skin has bonded well with it. The level of porosity in the metallic microstructure is as low as $1.9 \pm 1.3\%$.

Figure 3 shows examples of heat exchangers made by spray forming. The first is a flat nickel sheet, $220 \times 100 \times 10$ mm^3 in size (Fig. 3(*a*)), with a metal coating sprayed on all sides. The second sample is a cylindrical section 200 mm long and 80 mm wide with both metal and ceramic coatings. The two ends of the foam sheets were not coated but covered with custom made stainless steel end caps sealed in place with a high-temperature adhesive (Aremco Products Inc., Valley Cottage, NY). Hose fittings were installed in the end caps to attach tubes for airflow.

(*a*) (*b*)

Fig. 1 (*a*) 20 PPI nickel foam and (*b*) nickel foam with ceramic (lower sample) or metallic coating (upper sample)

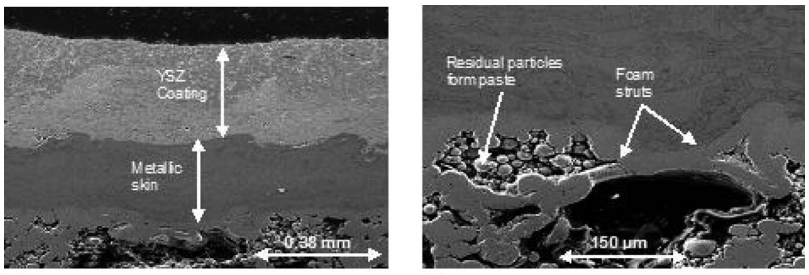

(*a*) (*b*)

Fig. 2 SEM micrographs of the metallic skin deposited by wire-arc spraying and YSZ deposited by APS

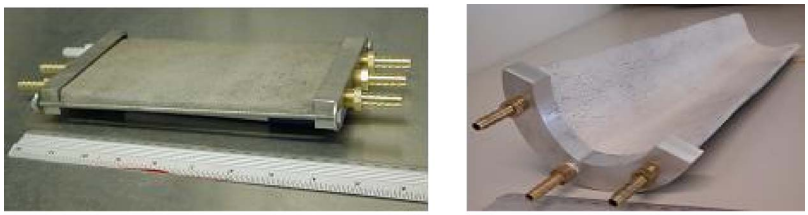

(*a*) (*b*)

Fig. 3 10 mm thick, 10 PPI nickel foam with end caps attached in the shape of (*a*) a flat plate and (*b*) a section of a cylinder

3 Experimental Method

Figure 4 shows a schematic diagram of the apparatus used to measure both hydraulic and heat-transfer characteristics of flat foam heat exchangers. A copper heating plate 200×100 mm^2 in size was placed under the heat exchanger. Five 200 W cartridge heaters were inserted into the plate, regulated by a temperature controller. The hot plate temperature was adjusted so as to keep the temperature of the heat exchanger surface in contact with it uniform and constant, as measured by a *K*-type thermocouple. The hot side temperature of the heat exchanger was varied from 100°C to 500°C in increments of 100°C.

A mass flow meter was used to control and measure the coolant flow rate passing throughout the heat exchanger. The inlet coolant pressure was kept constant at 80 MPa for all experiments. The lowest flow rate was 5 l/min, which corresponds to a flow velocity of 0.1 m/s for a channel cross-section of 100×10 mm^2. The highest flow rate was 110 l/min, which corresponds to a flow velocity of 1.8 m/s for a channel cross-section of 100×10 mm^2. Pressure taps were inserted at the flow inlet and outlet to measure static pressure. A differential pressure transducer (PX142-005D5V, Omega Inc., Stamford, CT), was used to record the pressure drop with an accuracy of ±0.001 bar.

The inlet and outlet temperatures of the coolant were measured by two *K*-type thermocouples with an accuracy of ±1°C during experiments. Three more *K*-type thermocouples were attached to the cold side (upper surface) of the heat exchanger at three different positions; close to the inlet, middle of the length, and close to the outlet.

To test the sandwich structure under burner rig condition, a cylindrical section 200 mm long and 80 mm wide was made with 10 PPI foam in the core (Fig. 3(*b*)). Wire arc spraying was used to deposit metal coatings on both faces and a ceramic coating was plasma sprayed over the metal on the inner surface. The two ends of the section were not coated and an aluminum end caps was machined and sealed in place with a high-temperature adhesive (Aremco Products Inc., Valley Cottage, NY) on one end that served as the cooling air inlet. Three hose fittings were installed in the end cap to attach tubes for airflow. Three thermocouples were attached to the outer surface of the cylinder, close to the air inlet, middle, and outlet, respectively. Two more thermocouples were use to measure the inlet and outlet temperature of the coolant air.

Tests were done with the center of the ceramic-coated face directly exposed to a flame from a premixed methane-air burner (Fig. 5). The cylindrical flame had a diameter of 25 mm and a temperature of approximately 1400°C. The heat exchanger was cooled with an airflow rate of 100 l/min passed through the foam. The temperature of the outer (cold) side was measured using *K*-type thermocouples at three points: near the air inlet, at a point directly in line with the flame impingement point, and near the air outlet All thermocouples were connected to a data acquisition system and 100 samples per minute were recorded during experiments. Inner (hot) surface temperatures were measured at two points: the hottest point, directly where the flame impinged, and near the air outlet, using a pyrometer (Micron, M90, Micron Instrument Co., Inc., NJ).

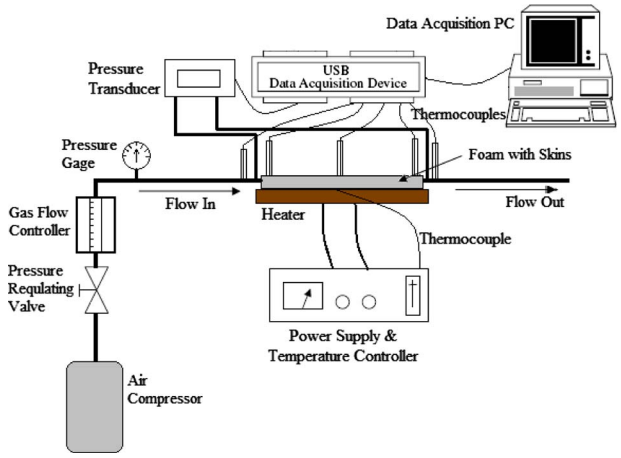

Fig. 4 Schematic of the experimental apparatus used to measure the characteristics of the skin coated nickel foam heat exchangers

4 Results and Discussion

4.1 Hydraulic Characteristics. Previous studies of flow through foam [7,8,13] have shown that it can be modeled as a porous medium and the pressure drop across it is a function of average flow velocity, that can be modeled by the equation

$$\frac{\Delta P}{L}=\frac{\mu}{K}V+\rho CV^2 \tag{1}$$

where ΔP is the pressure drop across the foam, L is the length of the heat exchanger, ρ and μ are the density and dynamic viscosity of the coolant fluid, respectively (for air, $\rho=1.205$ kg/m^3 and μ

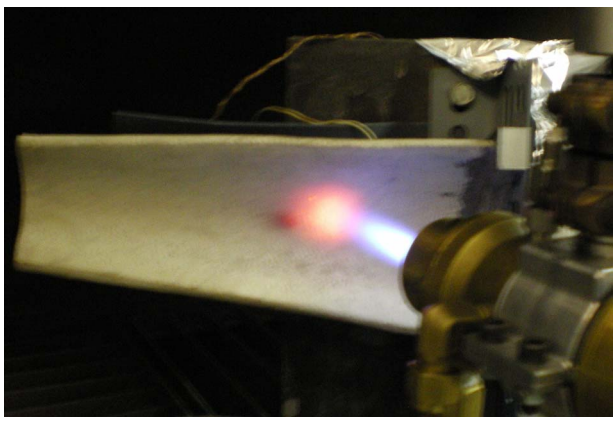

Fig. 5 Burner rig experiment set up

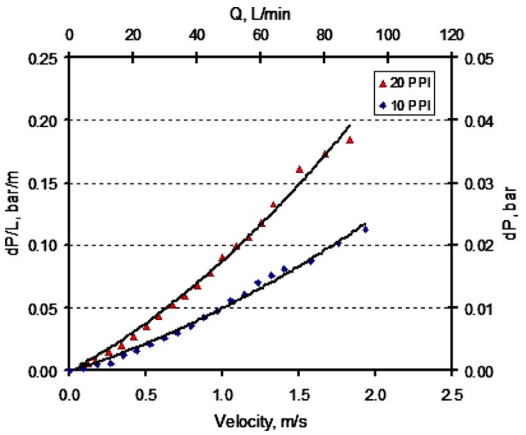

Fig. 6 Variation in pressure drop with air velocity for the 10 and 20 PPI nickel foam heat exchangers

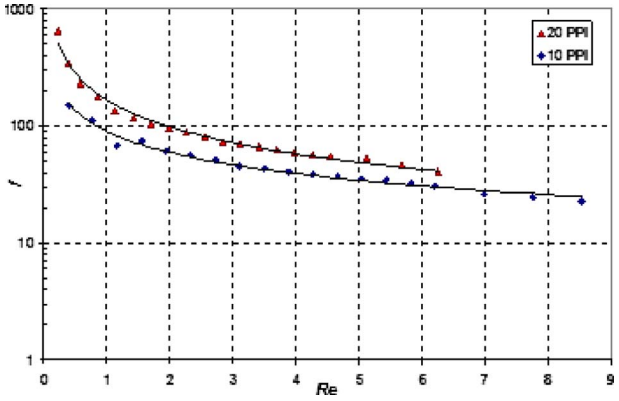

Fig. 7 Variation in Fanning friction factor *f* with Re number for 10 and 20 PPI foam heat exchangers

$=1.888\times10^{-5}$ kg/ms). V is the Darcian velocity defined as the volume flow rate of fluid per unit cross-section area of the channel (ignoring the foam). Two constants describe the geometry of the foam: the permeability K (with units m^2) and the form coefficient of the foam C (m^{-1}), which are a function of pore size, geometry, and density.

Figure 6 shows the pressure drops and pressure gradients across 220 mm long, 100 m wide, and 10 mm thick heat exchangers made from 10 and 20 PPI nickel foam. The volume flow rate of air was varied from 0 l/m to 100 l/m, measured at standard temperature and pressure (0°C, atmospheric pressure) giving average flow velocities from 0 m/s to approximately 2 m/s. Fitting Eq. (1) to the experimental data, we calculated $K=4.9\times10^{-9}$ m^2 and $C=954$ m^{-1} for the 10 PPI foam and $K=2.9\times10^{-9}$ m^2 and $C=1892$ m^{-1} for the 20 PPI foam. Curves of best fit are shown in Fig. 6.

The Reynolds number for flow through foam has been defined as [7]

$$\mathrm{Re}=\frac{\rho V\sqrt{K}}{\mu} \tag{2}$$

where the appropriate length scale is the $\sqrt{K}$.

The pressure drop can be represented in nondimensional form as the Fanning friction factor f defined as [2]

$$f=\frac{\Delta P}{4\left(\frac{L}{D_h}\right)\left(\frac{\rho V^2}{2}\right)} \tag{3}$$

where D_{hyd} is the hydraulic diameter of the flow channel

$$D_h=\frac{4A_c}{L_p} \tag{4}$$

A_c is the cross sectional area of the flow channel ($A_c=1000$ mm^2) and L_p is the wetted perimeter of the flow channel ($L_p=220$ mm). Therefore, the hydraulic diameter of the heat exchanger is 0.018 m.

Figure 7 shows the friction factors for both 10 and 20 PPI foam heat exchangers calculated from Eq. (4) as a function of Re. The friction factor first decreases rapidly with increasing Re and then approaches a constant value. As flow velocity increases the second term in Eq. (1), proportional to V^2, becomes dominant so that

$$\frac{\Delta P/L}{\rho V^2}\approx C \tag{5}$$

and f becomes constant.

The experimental friction factor data can be correlated by an equation of the form

$$f=\frac{C_1}{\mathrm{Re}}\quad \text{for}\ \mathrm{Re}>4 \tag{6}$$

where $C_1=190$ for the 10 PPI foam and $C_1=250$ for the 20 PPI foam. These curves of best fit are shown in Fig. 7.

4.2 Heat Transfer Characteristics. Figure 8 shows the temperature increase (T_o-T_i) of air passing through the 20 PPI foam heat exchanger while its bottom surface was heated to temperatures ranging from 100–500°C and flow velocity was varied from 0 m/s to 1.8 m/s. The inlet velocity in all cases was approximately $T_i=25$°C. The outlet fluid temperature (T_o) increased with flow velocity, reaching a plateau above $V=0.7$ m/s ($Q=40$ l/min). At the highest face temperature (500°C) the air was heated by 140°C.

There were large temperature differences between the bottom surface of the heat exchanger, in contact with the heater block, and the upper surface that was exposed to ambient air. Figure 9 shows temperature differences ($\Delta T=T_h-T_c$) between the hot side (T_h) and cold side (T_c) of the 20 PPI foam heat exchanger as a function of flow velocity at various hot side temperatures. T_h remains uniform since it is in contact with the heater plate. T_c increases from the inlet to the outlet; we used the value of T_c measured near the air inlet of the heat exchanger. The temperature of

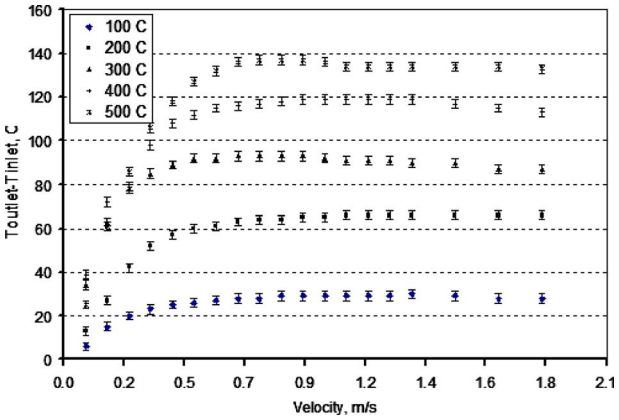

Fig. 8 Increase in air temperature flowing through the 20 PPI foam heat exchanger at various coolant flow velocities. Inlet temperature was approximately 25°C.

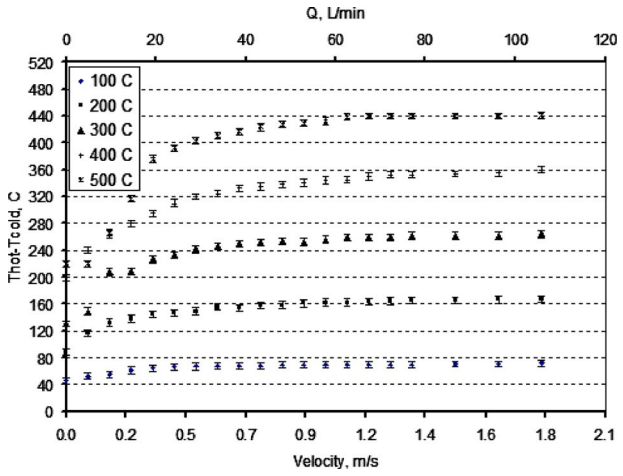

Fig. 9 Temperature differences between the hot side and cold side of the 20 PPI foam heat exchanger at various hot side temperatures

the cold side of the heat exchanger increased from only 30°C to 50°C when the temperature of the hot side was raised from 100°C to 500°C.

Figure 10 compares the performance of the 10 and 20 PPI foam heat exchangers at various coolant flow velocities with the hot surface temperature kept constant at 500°C. For a given air flow velocity, the outlet air temperature in the heat exchanger with 20 PPI foam in the core was about 20°C higher that that for the heat exchanger with 10 PPI foam, indicating higher heat-transfer. The 20 PPI foam had smaller pore diameter and larger internal heat-transfer area. The cold surface temperature in a 20 PPI foam heat exchanger was approximately 30°C less than that for the 10 PPI foam heat exchanger under the same test condition.

Heat-transfer in a heat exchanger is characterized by the dimensionless Nusselt number [2].

$$\mathrm{Nu} = \frac{hD_{\mathrm{hyd}}}{k_C} = \frac{q}{A_h \Delta T}\frac{D_{\mathrm{hyd}}}{k} \tag{7}$$

where h is the convection heat-transfer coefficient, k is the thermal conductivity of air, and q the heat-transfer rate to the air. A_h is the heat-transfer area, taken to be the area of contact between the heat exchanger and the heater plate (0.022 m^2) [2]. The temperature difference ΔT was taken as the difference between the hot side of the heat exchanger and inlet fluid temperature $\Delta T = T_h - T_i$.

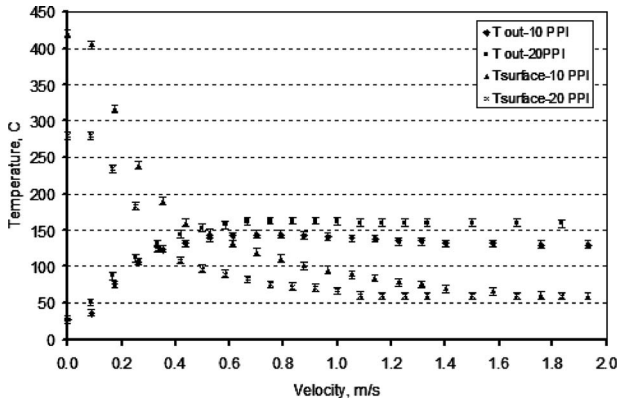

Fig. 10 Outlet air temperature and heat exchanger cold side temperature for the 10 and 20 PPI foam heat exchangers at various air flow velocities. The hot surface temperature was kept constant at 500°C.

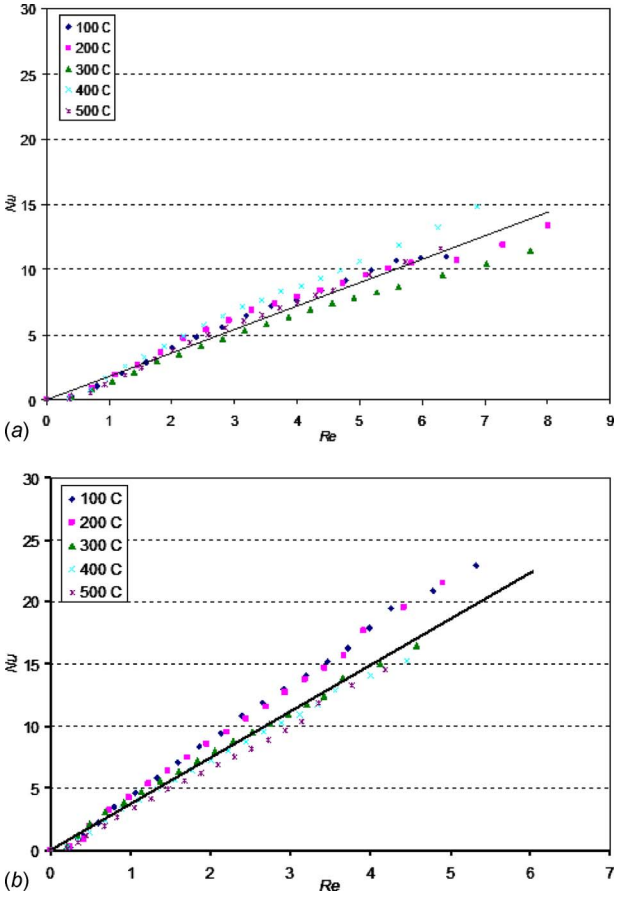

Fig. 11 Variation in Nusselt number with coolant flow velocities at various hot side temperatures in (*a*) 10 PPI foam heat exchanger and (*b*) 20 PPI foam heat exchanger

The heat-transfer to the air can be calculated from the energy balance

$$q = \dot{m} \cdot c_p (T_o - T_i) \tag{8}$$

where $\dot{m}$ is the mass flow rate of the coolant and c_p is the specific heat of air. Substituting Eq. (8) into Eq. (7), Nu can be calculated from

$$\mathrm{Nu} = \frac{m \cdot c_p (T_o - T_i)}{A_h (T_h - T_i)}\frac{D_{\mathrm{hyd}}}{k} \tag{9}$$

The variations in the Nusselt number, Nu, obtained from Eq. (9) at various coolant flow velocities for the heat exchangers with 10 PPI and 20 PPI foam in the core, when the hot side of the heat exchangers was kept at constant temperatures, are plotted in Fig. 11. Air properties were evaluated at the average temperature $(T_i + T_o)/2$. Nu reached a maximum of almost 15 in the 10 PPI foam heat exchanger and 25 in the 20 PPI foam at the highest air velocity, 1.8 m/s (110 l/min). For a given coolant flow velocity and hot plate temperature Nu for the heat exchanger with 20 PPI foam in the core was approximately 80% higher than that for the heat exchanger with 10 PPI foam in the core.

The experimental data for a 10 PPI foam heat exchanger were correlated by a linear fit.

$$\mathrm{Nu} = 1.8\ \mathrm{Re} \tag{10}$$

And for a 20 PPI heat exchanger

$$\mathrm{Nu} = 3.7\ \mathrm{Re} \tag{11}$$

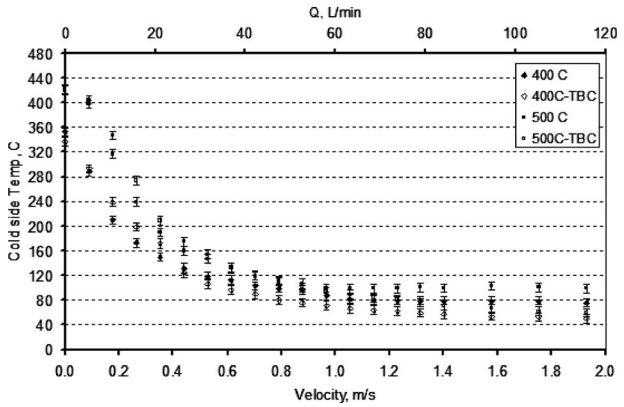

Fig. 12 Cold side temperature of the 10 PPI foam heat exchanger, with and without TBC, as a function of air velocity

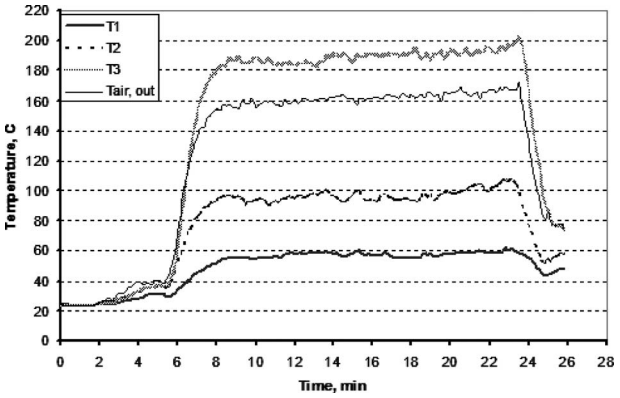

Fig. 13 Temperature variations versus time in the burner rig experiment. *T*1: temperature of back (cold) surface close to the entrance, *T*2: temperature of back surface opposite the flame impingement point, *T*3: temperature of back surface close to the exit, and $T_{air,out}$: temperature of the coolant air at exit.

Equations (10) and (11) are drawn in Figs. 11(*a*) and 11(*b*). They predict the experimental data within ± 0.3 and ± 0.3 for 10 and 20 PPI heat exchangers, respectively.

Applying a ceramic thermal barrier coating makes a heat exchanger surface more resistant to combustion gases since it reflects radiation, shields the metal surface from corrosion and reduces thermal shock due to sudden temperature changes. The coating also acts as an insulator, although this effect is relatively small since the coating thickness is typically only a fraction of a millimeter. The thermal resistance of the ceramic coating becomes significant only at large heat fluxes.

To determine the effect of a thermal barrier coating on the heat-transfer performance of the heat exchanger, the hot side of the flat 10 PPI foam heat exchanger was coated with a 300 μm layer of yttria stabilized zirconia. The ceramic-coated face was kept in contact with the heater plate and held at constant temperature during the experiments. Cold side temperatures were recorded while varying airflow rate. Figure 12 shows temperature variations of the cold side of the heat exchanger as a function of air velocity when the hot side temperature was kept at a constant temperature of either 400°C or 500°C. At low coolant flow, the TBC appeared to have no significant effect on heat-transfer. At high airflow rates the effect of the TBC on reducing the heat-transfer becomes apparent. When the hot plate was kept at 500°C, the cold side temperature was around 40°C lower with the TBC than without.

The increase in air temperature during a burner rig test with the ceramic-coated 10 PPI foam heat exchanger is shown in Fig. 13. Time $t=0$ corresponds to the burner being turned on. The flame was allowed to stabilize and then directed onto the face of the heat exchanger at $t=6$ min. Four temperatures are shown, that of the air leaving the heat exchanger and at three positions on the cold face. *T*1 was near the air inlet, *T*2 at the center, opposite the point at which the flame impinged, and *T*3 near the flame exit. The air temperature increased to approximately 160°C when the flame was turned on, and then remained constant. The temperature of the inner surface of the heat exchanger, where the flame impinged on it, was measured by a pyrometer as being 996°C. The surface temperature on the back surface of the heat exchanger varied between 180°C and 200°C near the air exit while the inner surface temperature at the same location was 550°C.

The analysis of heat exchanger for burner rig configuration is difficult since the applied heat flux is not uniformly distributed on the hot surface and the total energy input is not known. However, for the conditions of the flame test the calculated Re number using Eq. (2) was approximately 7 which correspond to Nu=13 from the correlation for the 10 PPI foam, given by Eq. (10). Substituting this value of Nu in Eq. (9) and the temperature differences between the inlet and outlet coolant flow ($T_o - T_i = 135$°C) obtained experimentally, the average temperature differences between the hot and cold side of the cylinder ($T_o - T_h$) is determined to be approximately 300°C. The measured temperature difference between the hot and cold side near the air exit was approximately 350°C, suggesting that the Nusselt number correlations can be used to design high-temperature heat exchangers.

The main purpose of the burner rig tests was to establish that the heat exchangers could survive prolonged contact with hot combustion products. After several test cycles in which the ceramic face was directly exposed to the burner flame for cycles for periods up to 30 min at a time the coatings showed no signs of damage, confirming that they are suitable for high-temperature applications.

5 Conclusion

Dense, strongly adhering skins of alloy 625 were deposited on the surfaces of 10 PPI and 20 PPI nickel foam sheets using twin wire-arc spraying to fabricate compact heat exchangers. Good mechanical contact was obtained between the skins and the foams struts, providing low thermal contact resistance. A ceramic coating was plasma sprayed over the metal coating on one face to provide resistance to high temperatures.

The experiments were carried out to characterize the hydraulic and thermal properties of the heat exchangers. The permeability and the form coefficient of both nickel foams (10 PPI and 20 PPI) in the core of the heat exchanger were determined at various coolant flow velocities. Correlations for the Fanning friction factor were obtained. Tests were done in which one face of the heat exchanger was held at constant temperature while the other was exposed to ambient air. The temperature rise of air flowing through the heat exchangers and the temperature difference between the hot and cold side were recorded. An energy balance was used to calculate average heat-transfer coefficients and the results expressed in dimensionless form. The Nusselt number for flow through a foam heat exchanger increased linearly with Reynolds number for the range of parameters tested: correlations were developed. The 20 PPI foam showed higher resistance to flow and greater heat-transfer than the 10 PPI foam because of its smaller pore size and larger internal surface area. The ceramic thermal barrier coating reduced heat-transfer although the effect was only significant at high airflow rates, where heat flux was large.

Burner rig test tests were carried out in which the ceramic-coated face of the heat exchanger was directly exposed to a methane-air flame. The heat exchanger surface directly under the flame reached temperatures approaching 1000°C but sustained no damage after being repeatedly exposed for 25–30 min long periods.

References

[1] Banhart, J., 2001, "Manufacture, Characterization and Application of Cellular Metals and Metal Foams," Prog. Mater. Sci., **46**, pp. 559–632.

[2] Boomsma, K., Poulikakos, D., and Zwick, F., 2003, "Metal Foams as Compact High Performance Heat Exchangers," Mech. Mater., **35**, pp. 1161–1176.

[3] Hetsroni, G., Gurevich, M., and Rozenblit, R., 2005, "Metal Foam Heat Sink for Transmission Window," Int. J. Heat Mass Transfer, **48**, pp. 3793–3803.

[4] Xu, J. L., Ji, X. B., Zhang, W., and Liu, G. H., 2008, "Pool Boiling Heat Transfer of Ultra-Light Copper Foam With Open Cells," Int. J. Multiphase Flow, **34**, pp. 1008–1022.

[5] Vijaykant, S., and Agrawal, K. A., 2007, "Liquid Fuel Combustion Within Silicon-Carbide Coated Carbon Foam," Exp. Therm. Fluid Sci., **32**, pp. 117–125.

[6] Koltsnkis, G. C., Katsaounis, D. K., Samaras, Z. C., Naumann, D., Saberi, Sh., and Bohm, A., 2006, "Filtration and Regeneration Performance of a Catalyzed Metal Foam Particulate Filter," SAE Paper No. 2006-01-1524.

[7] Boomsma, K., and Poulikakos, D., 2001, "On the Effective Thermal Conductivity of a Three-Dimensionally Structured Fluid-Saturated Metal Foam," Int. J. Heat Mass Transfer, **44**, pp. 827–836.

[8] Dukhan, N., and Chen, K.-C., 2007, "Heat Transfer Measurements in Metal Foam Subjected to Constant Heat Flux," Exp. Therm. Fluid Sci., **32**, pp. 624–631.

[9] Gibson, L. J., and Ashby, M. F., 1988, *Cellular Solids, Structure & Properties*, Pergamon, Oxford, England.

[10] Salimijazi, H. R., Pershin, L., Coyle, T. W., Mostaghimi, J., and Chandra, S., 2008, *International Thermal Spray Conference & Expositions 2008: Thermal Spray Crossing Borders*, B. R. Marple, M. M. Hyland, Y.-C. Lau, C.-J. Li, R. S. Lima, and G. Montavon, eds., ASM International, Maastricht, The Netherlands, Jun. 2–4, CD-ROM, pp. 230–235.

[11] Saaedi, J., Coyle, T. W., Mirdamadi, S., Arabi, H., and Mostaghimi, J., 2008, "Phase Formation in a Ni-50Cr HVOF Coating," Surf. Coat. Technol., **202**, pp. 5804–5811.

[12] Azarmi, F., Saaedi, J., Coyle, T. W., and Mostaghimi, J., 2008, "Microstructure Characterization of Alloy 625 Deposited on Nickel Foam Using Air Plasma Spraying," Adv. Eng. Mater., **10**(5), pp. 459–465.

[13] Fourar, M., Radilla, G., Lenormand, R., and Moyne, C., 2004, "On the Non-Linear Behavior of a Laminar Single-Phase Flow Through Two and Three-Dimensional Porous Media," Adv. Water Resour., **27**, pp. 669–677.